Available online at www.sciencedirect.com
SCIENCE DIRECT
Surface Science 600 (2006) 1804–1808
SURFACE SCIENCE
www.elsevier.com/locate/susc

Nucleation of ordered Fe islands on $Al_2O_3/Ni_3Al(1\,1\,1)$

A. Lehnert [a], A. Krupski [b,c,*], S. Degen [b], K. Franke [a], R. Decker [a], S. Rusponi [a], M. Kralj [b,1], C. Becker [b], H. Brune [a], K. Wandelt [b]

[a] Institut de Physique des Nanostructures, Ecole Polytechnique Fédérale de Lausanne (EPFL), CH-1015 Lausanne, Switzerland
[b] Institute of Physical and Theoretical Chemistry, University of Bonn, Wegelerstr. 12, D-53115 Bonn, Germany
[c] Institute of Experimental Physics, University of Wrocław, pl. Maksa Borna 9, 50-204 Wrocław, Poland

Received 20 October 2005; accepted for publication 8 February 2006
Available online 2 March 2006

Abstract

Scanning tunneling microscopy (STM) has been used to investigate the nucleation and stability of iron clusters on the $Al_2O_3/Ni_3Al(1\,1\,1)$ surface as a function of coverage and annealing temperature. We show that atomic beam deposition of iron leads to hexagonally ordered cluster arrangements with a distance of 24 Å between the clusters evidencing the template effect of the alumina film. The shape of the iron clusters is two-dimensional (2D) at deposition temperatures from 130 K to 160 K and three-dimensional (3D) at 300 K. However, the 2D iron clusters grown between 130 K and 160 K are stable up to 350 K.

Keywords: Aluminium; Nickel; Alumina; Iron; Scanning tunneling microscopy (STM); Cluster growth and nucleation

1. Introduction

Metal–oxide interfaces are of great interest for technological applications including metal–ceramic sensors, microelectronics, spintronic devices and oxide supported transition metal catalysts [1–6]. In this work we focus on the creation of small oxide supported iron clusters serving as a model system to investigate the catalytic and magnetic properties of nanosized metallic particles on an insulating substrate.

The catalytic properties of Fe clusters on oxides are of particular interest with regard to nitrogen fixation being of vital importance in biological systems and of highest relevance in technological processes [7]. Biological nitrogen fixation was the subject of numerous experimental as well as theoretical studies aiming at a detailed picture of the catalytically active part in an enzyme and of the reaction pathway [8–10]. A recent publication dealing with small Fe clusters on MgO(1 0 0) attributes to this model system catalytic properties similar to the active site in the biological enzyme nitrogenase [11].

The effects of the reduced particle size and of the insulating substrate are not only crucial for the catalytic activity, they are expected to introduce also new physical properties. Of particular interest are the magnetic properties of the small iron particles supported by oxide systems with respect to the development of high-density magnetic data recording devices [12,13]. Density functional calculation revealed that small Fe_n clusters ($n \leqslant 8$) deposited on an inert substrate have magnetic moments largely exceeding the Fe bulk value [14], which is consistent with the same observation for metal clusters in the gas phase [15].

Recently, it was also shown that metal deposition on $Al_2O_3/Ni_3Al(1\,1\,1)$ may lead to ordered cluster arrays [16,17]. In the present paper, we report on an STM study of the growth of Fe clusters on $Al_2O_3/Ni_3Al(1\,1\,1)$ by iron

* Corresponding author. Address: Institute of Experimental Physics, University of Wrocław, pl. Maksa Borna 9, 50-204 Wrocław, Poland. Tel.: +48 71 375 9459; fax: +48 71 328 7365.
E-mail addresses: akrupski@thch.uni-bonn.de, akrupski@ifd.uni.wroc.pl (A. Krupski).
[1] Permanent address: Institute of Physics, Bijenicka c.46, PO Box 304, 10000 Zagreb, Croatia.

0039-6028/$ - see front matter © 2006 Elsevier B.V. All rights reserved.
doi:10.1016/j.susc.2006.02.013

vapor deposition as a function of coverage and annealing temperature.

2. Experiment

The experiments were performed in two different UHV chambers, each with a base pressure below 2×10^{-8} Pa. The $Ni_3Al(1\,1\,1)$ single crystal samples were supplied by MaTeck, Jülich. In this paper, the STM measurements presented in Figs. 1, 2(a) and 4 were done in Bonn using a homebuilt liquid helium cooled beetle type STM [18]. The main components of this low temperature (LT) STM are a copy of the original design by Stipe et al. [19]. The two other STM images (Figs. 3 and 5(a)) were taken in Lausanne with a homebuilt variable temperature (VT) STM [20,21]. For the preparation of the clean $Ni_3Al(1\,1\,1)$ surface and of the alumina film we followed the procedure described in Ref. [22]. For the LT-STM experiment iron (99.998%) was evaporated from an alumina crucible surrounded by a tungsten resistive heater and the coverage of iron was determined via STM. In case of the VT-STM experiment iron was evaporated with an e-beam evaporator from a pure iron rod (99.995%). The iron flux has been calibrated by means of Auger electron spectroscopy (AES) by relating the peak-to-peak height of the iron LMM transition at 705 eV to the transitions of the two substrate elements, namely the nickel LMM transition located at 849 eV, and the aluminium KLL transition at 1396 eV. Taking the substrate composition into account, this leads to iron evaporation fluxes of 0.37 ± 0.04 ML min^{-1} and 0.32 ± 0.04 ML min^{-1}, respectively. The values agree within the error bars, and we deduce a flux of 0.35 ± 0.06 ML min^{-1} after depositing several MLs. One ML of Fe clusters is defined as a Fe(1 1 0) plane of one atomic height (1.87×10^{15} atoms/cm^2). This is in good agreement with the flux of 0.40 ± 0.10 ML min^{-1} determined from STM images of the Fe islands considering tip convolution effects. For the AES calibration of the deposition flux we took the solid angle of the escaping electrons into account, leading to a by 10% reduced inelastic mean-free path [23]. All STM images were recorded in the constant current mode. The bias voltage has been applied to the sample with respect to the STM tip, which remained on virtual ground provided by the *I–V* converter. Some of the presented STM images were weakly filtered using a Fourier filter. The STM data were processed using a freeware image processing software [24].

3. Results and discussion

3.1. The $Al_2O_3/Ni_3Al(1\,1\,1)$ surface

Recent SPA-LEED and STM investigations showed, that the Al_2O_3 film forms a long-range ordered superstructure on the nanometer scale [22,25]. The strong dependence of the corrugation imaged by STM one can see in Fig. 1(a) and (b) and in the lower part of Fig. 2(a). At bias voltages around $U_{bias} = 3.2$ V, see Fig. 1(a), one sees a hexagonal arrangement of hollows (points B) where every hollow is surrounded by a hexagonal ring of brighter spots. This structure possesses an apparent lattice constant of 24 Å (between hollow sites) and will be referred to as "network structure" in the following. However, a closer inspection of this structure indicates that not all hollows have the same depth. Some hollows are by 40 Å shallower than the others [22]. The shallower hollows (points A in Fig. 1) form a regular arrangement, which forms the basis of the hexagonal unit cell (marked in Figs. 1 and 2(a)) with lattice vectors of 41.6 Å [22]. The unit cell of the alumina film is more easily seen in the STM images in Fig. 1(b) and 2((a) lower part) due to a contrast reversal [26], which is found between the bias voltages of 2.0 and 4.2 V, and will be referred to as "dot structure" in the following.

3.2. The $Fe/Al_2O_3/Ni_3Al(1\,1\,1)$ system

The iron clusters grow and gradually cover the entire $Al_2O_3/Ni_3Al(1\,1\,1)$ surface with increasing coverage.

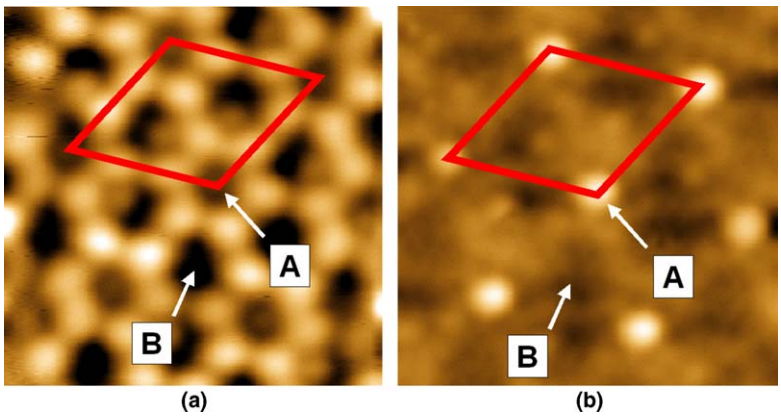

Fig. 1. STM images (105 Å × 105 Å; $I_T = 71$ pA; $T_{STM} = 23$ K) of the $Al_2O_3/Ni_3Al(1\,1\,1)$ measured at $U_{bias} = 3.2$ and 2.0 V (a) and (b), respectively. The unit cell of the "dot structure" is marked. Labels A and B are on two characteristic points imaged differently in the alumina film (see text).

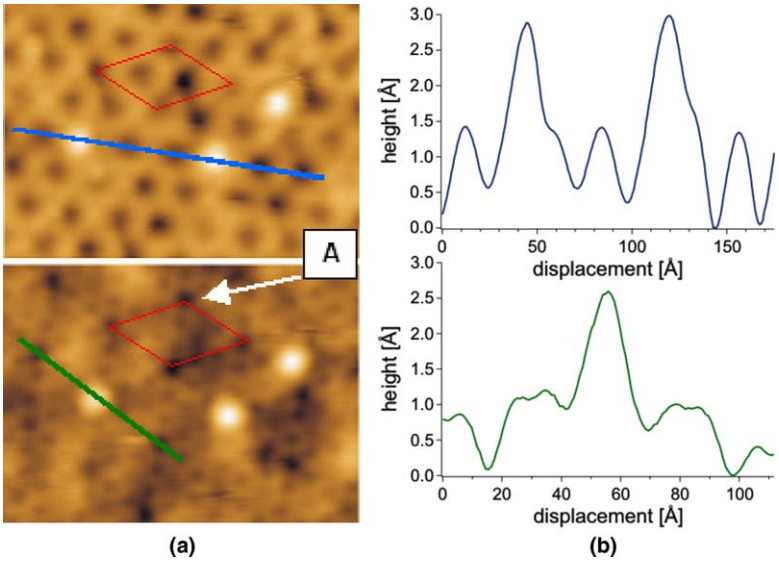

Fig. 2. (a) STM images of Fe clusters on $Al_2O_3/Ni_3Al(1\,1\,1)$ deposited at 160 K ($\Theta = 0.07 \pm 0.02$ ML; 198 Å × 98 Å; $I_T = 106$ pA; $U_{bias} = 3.5$ and 4.2 V in upper and lower part, respectively; $T_{STM} = 23$ K). The unit cell of the "dot structure" is marked. The label A shows the same characteristic point as in Fig. 1. (b) Corresponding line profiles along the white lines in the left hand images.

However, the growth of a continuous wetting layer of Fe has not been observed. This result is in agreement with the thermodynamic criterion for the wetting of alumina [27–29]. From energetic considerations wetting does not occur on the alumina surface if $E_{adh} < 2\gamma_{v/m}$, where E_{adh} is the adhesion and $\gamma_{v/m}$ is the surface free energy at the vacuum metal interface for the liquid metal. E_{adh} is the energy needed to separate the metal and the oxide at their interface resulting in the bare oxide surface. $E_{adh} = 1205$ mJ/m^2 was measured for iron on alumina at 1853 K [29]. E_{adh} is mainly energetic and therefore nearly temperature independent. $\gamma_{v/m}$ ($T = 1853$ K) = 1787 mJ/m^2 can be extrapolated to temperatures below the phase transition entailing an increasing $\gamma_{v/m}$ [27,29]. The thermodynamic criterion (no wetting) is consistent with the observation of three-dimensional (3D) particles at 300 K.

3.2.1. Iron deposition at a sample temperature between 130 K and 160 K

In Figs. 2–4 the iron clusters grown at a low deposition temperature (130 K–160 K) are depicted. The situation for low iron coverage ($\Theta = 0.07 \pm 0.02$ ML) is shown in Fig. 2(a). The iron clusters appear as bright spots on top of the long-range modulated alumina film. As evidenced in the upper part taken at $U_{bias} = 3.5$ V, the iron clusters nucleate in the hollows corresponding to points B ("network structure") of the alumina film. A similar behavior was observed for V and Mn [16] on the same kind of film. The noble metals Ag, Cu, Au and Pd, however, nucleate

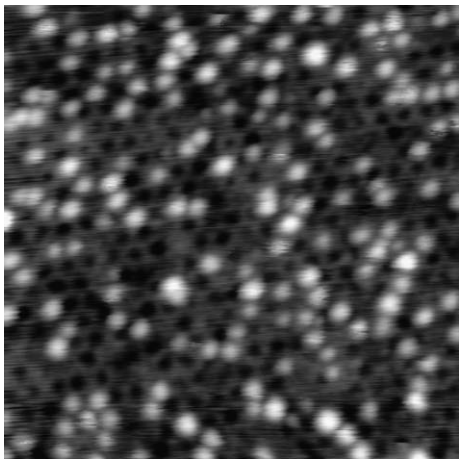

Fig. 3. STM image of Fe clusters on $Al_2O_3/Ni_3Al(1\,1\,1)$ deposited at 140 K ($\Theta = 0.09 \pm 0.03$ ML; 400 Å × 400 Å; $I_T = 135$ pA; $U_{bias} = 3.5$ V; $T_{STM} = 140$ K).

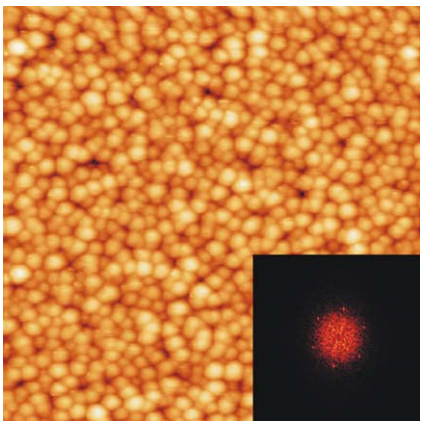

Fig. 4. STM image of Fe clusters on $Al_2O_3/Ni_3Al(1\,1\,1)$ deposited at 130 K ($\Theta = 1.0 \pm 0.2$ ML; 681 Å × 681 Å; $I_T = 78$ pA; $U_{bias} = 0.7$ V; $T_{STM} = 300$ K). The FFT shown in the inset evidences a hexagonal arrangement of the iron clusters with a nearest neighbor distance of 24 Å.

preferentially on the "dot structure" (points A) of Al_2O_3/$Ni_3Al(1\,1\,1)$ being 41.6 Å apart [16,17]. The apparent height of the iron clusters grown between 130 K and 160 K amounts to 2.6 ± 0.3 Å with respect to the oxide surface, as inferred from the line profile shown in Fig. 2(b). A large area scan for an iron coverage of $\Theta = 0.09 \pm 0.03$ ML is shown in Fig. 3. Again, the Fe clusters are located on the "network structure" of the alumina film. In some cases they occupy neighboring sites, which are only 24 Å apart without coalescing. From a comparison of the coverage determination with AES to the area covered by Fe as determined by STM we conclude that the islands are one atomic layer in height. A second argument for two-dimensional (2D) clusters comes from the significantly larger apparent height for the 3D clusters to be discussed below.

Cluster growth is a non-equilibrium process and the final *macroscopic* state of the system depends on the different activation energies for all *microscopic* kinetic processes being involved. At 130 K, respectively 160 K, the growth is limited to 2D, since a diffusing Fe atom laterally approaching a 2D island attaches to the step but cannot climb up on the island's top. However, an Fe atom landing on-top of an Fe island can overcome the Ehrlich–Schwoebel barrier and moves down-step.

At an Fe coverage of $\Theta = 1.0 \pm 0.2$ ML the nucleation sites of the "network structure" are all filled with Fe clusters which partly coalesce (Fig. 4). From the Fourier transform (FFT) shown in the inset one can see a long-range hexagonal order of the iron clusters that corresponds to a distance of 24 Å between the clusters.

3.2.2. Iron deposition at a sample temperature of 300 K

For a deposition temperature of 300 K, the iron clusters populate again at the "network structure" of the superstructure, however, they are now three-dimensional. Now, an atom which encounters laterally an Fe island can step up on the island leading to a situation which is energetically favourable according to the reflection based on thermodynamics presented in Section 3.2. Fig. 5(a) shows the situation for a low iron coverage of $\Theta = 0.18 \pm 0.04$ ML. The upper part taken at $U_{bias} = 4.2$ V shows the long-range order of the alumina film and the iron clusters which are preferentially situated in the points B of the "network structure". The profile of the iron clusters shown in Fig. 5(b) reveals an apparent height of 7–8 Å which clearly indicates a 3D form of the iron clusters. Again, this is in agreement when comparing the AES derived coverage and the Fe covered area from STM images. Upon increasing the iron coverage the clusters remain separated. The formation of larger aggregates by coalescence has not been observed.

3.2.3. Iron cluster shape and stability

The iron clusters imaged at room temperature (Fig. 4) after having deposited iron at a sample temperature of 130 K are still two-dimensional which can be deduced from their apparent height of 2.6 ± 0.3 Å. In another experiment (not shown) the iron clusters grown at 150 K were annealed for 20 min at 350 K and STM images were again taken at 150 K. Equally, the apparent cluster height was the one we attribute to 2D islands. Thus, the shape of the iron clusters is determined by the sample temperature during deposition and remains unchanged during annealing to room temperature or even slightly above. This information on the stability is an important prerequisite when subsequently running catalytic reactions or investigating the temperature dependence of magnetic properties, such as the zero field susceptibility [30]. The fact that growth and annealing temperature have quite different influence on the cluster shape has been outlined for the case of Pd/MgO(1 0 0) in Ref. [2]. It is caused by the generally higher energy barrier required to transform an entire island into its equilibrium shape compared to the one required to put the atoms, coming in one by one during growth and being lower coordinated, onto thermodynamically favorable sites. Therefore islands may well remain 2D upon

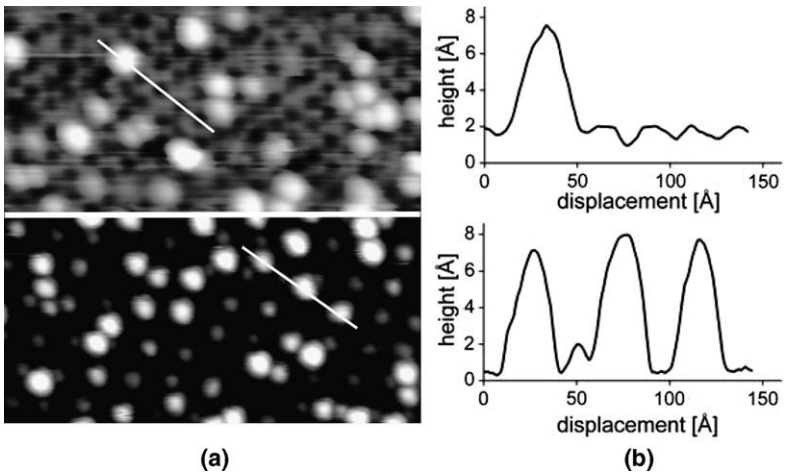

Fig. 5. (a) STM images of Fe clusters on $Al_2O_3/Ni_3Al(1\,1\,1)$ deposited and imaged at room temperature ($\Theta = 0.18 \pm 0.04$ ML; 400 Å × 200 Å; $I_T = 135$ pA; $U_{bias} = 4.2$ and 2.4 V in upper and lower part, respectively). (b) corresponding line profiles along the white lines in the left hand images.

annealing to temperatures higher than the growth temperature where they are 3D.

4. Conclusions

The STM results presented here indicate that the nucleation site of iron clusters on the $Al_2O_3/Ni_3Al(1\,1\,1)$ is largely independent of deposition temperature, while the cluster shape is, namely 2D in the range of 130–160 K and 3D at 300 K. At coverages close to one monolayer the Fe clusters form a regular hexagonal lattice with 24 Å spacing, and at low coverages they occupy only part of the available nucleation sites. In comparison with Mn and V cluster growth on the alumina film the observed perfection of the order of the clusters arrays increases from Mn- to Fe- to V-cluster arrays [16]. The iron clusters grown between 130 K and 160 K are stable against coarsening and shape changes upon prolonged annealing to temperatures up to 350 K.

Acknowledgments

A. Lehnert would like to acknowledge Dr. Carl Duisberg Stiftung for a fellowship. A. Krupski and M. Kralj are grateful to the Alexander von Humboldt and Hertie foundations for providing them with fellowships. Work of A. Krupski was supported by the University of Wrocław under Grant No. 2016/W/IFD/2006. The financial support by the Deutsche Forschungsgemeinschaft (DFG) through SFB 624 is gratefully acknowledged.

References

[1] C.T. Campbell, Surf. Sci. Rep. 27 (1997) 1.
[2] C.R. Henry, Surf. Sci. Rep. 31 (1998) 231.
[3] M. Bäumer, H.J. Freund, Prog. Surf. Sci. 61 (1999) 127.
[4] S.A. Chambers, Surf. Sci. Rep. 39 (2000) 105.
[5] A.K. Santra, D.W. Goodman, J. Phys.: Condens. Matter 15 (2002) R31.
[6] S.A. Wolf, D.D. Awschalom, R.A. Buhrman, J.M. Daughton, S.v. Molnár, M.L. Roukes, A.Y. Chtchelkanova, D.M. Treger, Science 294 (2001) 1488.
[7] G. Ertl, H.J. Freund, Phys. Today 52 (1999) 32.
[8] J.B. Howard, D.C. Rees, Chem. Rev. 96 (1996) 2965.
[9] B.K. Burgess, D.J. Lowe, Chem. Rev. 96 (1996) 2983.
[10] B. Hinnemann, J.K. Nørskov, J. Am. Ceram. Soc. 126 (2004) 3920.
[11] Z. Sljivancanin, A. Pasquarello, Phys. Rev. B 71 (2005) 081403.
[12] M.L. Plumer, J.v. Ek, D. Weller (Eds.), The Physics of Ultra-High-Density Magnetic Recording, Springer, Berlin, 2001.
[13] S.D. Bader, Surf. Sci. 500 (2002) 172.
[14] Z. Sljivancanin, A. Pasquarello, Phys. Rev. Lett. 90 (2003) 247202.
[15] I.M.L. Billas, A. Châtelain, W.A.d. Heer, Science 265 (1994) 1682.
[16] C. Becker, A. Rosenhahn, A. Wiltner, K.V. Bergmann, J. Schneider, P. Pervan, M. Milun, M. Kralj, K. Wandelt, New J. Phys. 4 (2002) 75.
[17] S. Degen, C. Becker, K. Wandelt, Faraday Discuss. 125 (2004) 343.
[18] K. Besocke, Surf. Sci. 181 (1987) 145.
[19] B.C. Stipe, M.A. Rezaei, W. Ho, Rev. Sci. Instrum. 70 (1999) 137.
[20] H. Brune, H. Röder, K. Bromann, K. Kern, Thin Solid Films 264 (1995) 230.
[21] N. Weiss, Propriétés Magnétiques de Nanostructures de Cobalt Adsorbées, Lausanne, EPFL, 2004.
[22] S. Degen, A. Krupski, M. Kralj, A. Langner, C. Becker, M. Sokolowski, K. Wandelt, Surf. Sci. 576 (2005) L57.
[23] D. Briggs, J.T. Grant, Surface Analysis by Auger and X-Ray Photoelectron Spectroscopy, IM Publications and Surface Spectra Limited, West Sussex, 2003.
[24] WSXM©. Available from: <http://www.nanotec.es>.
[25] S. Degen, A. Krupski, M. Kralj, C. Becker, K. Wandelt, before submission.
[26] T. Maroutian, S. Degen, C. Becker, K. Wandelt, R. Berndt, Phys. Rev. B 68 (2003) 155414.
[27] A.W. Adamson, Physical Chemistry of Surfaces, Wiley, New York, 1990.
[28] D. Chatain, L. Coudurier, N. Eustathopoulos, Rev. Phys. Appl. 23 (1988) 1055.
[29] D. Chatain, I. Rivollet, N. Eustathopoulos, J. Chim. Phys. 83 (1986) 561.
[30] S. Rusponi, T. Cren, N. Weiss, M. Epple, P. Buluschek, L. Claude, H. Brune, Nat. Mater. 2 (2003) 546.